Recruitment of the NineTeen Complex to the activated spliceosome requires AtPRMT5

Xian Deng[a,1], Tiancong Lu[a,1], Lulu Wang[a,1], Lianfeng Gu[a], Jing Sun[a], Xiangfeng Kong[a], Chunyan Liu[a,2], and Xiaofeng Cao[a,b,2]

[a]State Key Laboratory of Plant Genomics and National Center for Plant Gene Research, CAS Center for Excellence in Molecular Plant Sciences, Institute of Genetics and Developmental Biology, Chinese Academy of Sciences, Beijing 100101, China; and [b]Collaborative Innovation Center for Genetics and Development, Fudan University, Shanghai 200438, China

Edited by Caroline Dean, John Innes Centre, Norwich, United Kingdom, and approved March 30, 2016 (received for review November 15, 2015)

Protein arginine methylation, catalyzed by protein arginine methyltransferases (PRMTs), is involved in a multitude of biological processes in eukaryotes. Symmetric arginine dimethylation mediated by PRMT5 modulates constitutive and alternative pre-mRNA splicing of diverse genes to regulate normal growth and development in multiple species; however, the underlying molecular mechanism remains largely unknown. A genetic screen for suppressors of an *Arabidopsis* symmetric arginine dimethyltransferase mutant, *atprmt5*, identified two gain-of-function alleles of pre-mRNA processing factor 8 gene (*prp8-8* and *prp8-9*), the highly conserved core component of the U5 small nuclear ribonucleoprotein (snRNP) and the spliceosome. These two *atprmt5 prp8* double mutants showed suppression of the developmental and splicing alterations of *atprmt5* mutants. In *atprmt5* mutants, the NineTeen complex failed to be assembled into the U5 snRNP to form an activated spliceosome; this phenotype was restored in the *atprmt5 prp8-8* double mutants. We also found that loss of symmetric arginine dimethylation of Sm proteins prevents recruitment of the NineTeen complex and initiation of spliceosome activation. Together, our findings demonstrate that symmetric arginine dimethylation has important functions in spliceosome assembly and activation, and uncover a key molecular mechanism for arginine methylation in pre-mRNA splicing that impacts diverse developmental processes.

arginine methylation | protein arginine methyltransferase | AtPRMT5 | pre-mRNA splicing | Prp19C/NTC

Protein arginine methyltransferase 5 (PRMT5), a highly conserved type II protein arginine methyltransferase, transfers methyl groups to arginine residues, generating monomethylarginine and symmetric ω-N^G, N'^G-dimethylarginine (SDMA) (1–3). In mammals, PRMT5 methylates and interacts with diverse proteins, including histones and other proteins, and has long been implicated in the modulation of a variety of processes, such as transcriptional regulation, RNA metabolism (4), apoptosis (5), signal transduction (6), and germ cell development (7). Both loss-of-function and overexpression of *PRMT5* are fatal in mammals (8). AtPRMT5, the *Arabidopsis* homolog of PRMT5, regulates multiple aspects of plant growth and development, such as flowering time, growth rate, leaf morphology, sensitivity to stress conditions, and circadian rhythm, by modulating transcription, constitutive and alternative precursor mRNA (pre-mRNA) splicing of diverse genes (9–13). AtPRMT5 also mediates the symmetric arginine dimethylation of uridine-rich small nuclear ribonucleoproteins (U snRNPs) AtSmD1, D3, and AtLSm4 proteins, thus linking arginine methylation and splicing (10, 11, 13). However, the exact mechanism remains elusive.

Pre-mRNA splicing occurs in the nucleus, removing introns and ligating exons (14). In eukaryotes, most introns are spliced in a series of reactions catalyzed by the spliceosome, which consists of five subcomplexes of U snRNPs and several non-snRNP factors. Each U snRNP contains distinct splicing factors plus a uridine-rich small nuclear RNA (snRNA), namely U1, U2, U4, U5, or U6 (15). PRMT5 plays important roles in U snRNP assembly, in which U1, 2, 4, 5 snRNP Sm proteins Sm B/B′, D1, D3, and U6 snRNP-specific Sm-like protein LSm4 are symmetrically dimethylated by PRMT5 (16, 17). These methylated Sm proteins can be recognized by the survival motor neuron (SMN) complex or Tudor staphylococcal nuclease (Tudor-SN) and loaded onto U snRNAs, forming U snRNPs (18–20).

The snRNPs assemble dynamically on a pre-mRNA along with the non-snRNP splicing factors and catalyze two sequential transesterification reactions producing a mature mRNA. Briefly, U1 snRNP first recognizes the conserved 5′ splice site sequence in the intron by base pairing. U2 snRNP then binds the conserved branch-point sequence forming the prespliceosome. A preformed U4/U6.U5 tri-snRNP, in which the U4 and U6 snRNAs are base-paired, joins the prespliceosome to form the precatalytic spliceosome. A large structural rearrangement occurs to form an active spliceosome, involving the unwinding of U4/U6 base pairing interaction, the release of U1 and U4 snRNAs, and the addition of a non-snRNP protein complex called the Prp19 complex (Prp19C) or the NineTeen Complex (NTC) (21). Then the branch-point adenosine residue nucleophilically attacks the 5′ splice site for the first transesterification reaction, followed by the second transesterification reaction, resulting in the ligation of two exons. The spliceosome is a highly dynamic structure, assembled by sequential binding of the splicing factors to the pre-mRNA for each round of splicing, and then released for recycling after completion of the reaction (22).

From a genetic screen of second-site suppressors, we identified two neomorphic mutations in the core spliceosome component Prp8 (pre-mRNA processing factor 8) that suppress the pleiotropic

Significance

Protein arginine methyltransferase 5 (PRMT5) is involved in various developmental processes by globally regulating pre-mRNA splicing of diverse genes, but the underlying mechanism remains elusive. Here we demonstrate for the first time, to our knowledge, that *Arabidopsis* PRMT5 promotes the recruitment of the NineTeen Complex and splicing factors in the catalytic reactions to the spliceosome, thus promoting global pre-mRNA splicing. Our findings uncover a key molecular mechanism for PRMT5 in the regulation of pre-mRNA splicing, which fills a major gap in understanding of the role for PRMT5 in spliceosome assembly. Due to the conservation of PRMT5 in plants and animals, our finding is likely a fundamental molecular mechanism applicable to all eukaryotes, thereby shedding light on PRMT5 functions and spliceosome activation in animals.

Author contributions: X.D., T.L., L.W., C.L., and X.C. designed research; X.D., T.L., L.W., X.K., and C.L. performed research; X.D., L.G., J.S., C.L., and X.C. analyzed data; and X.D. and X.C. wrote the paper.

The authors declare no conflict of interest.

This article is a PNAS Direct Submission.

Freely available online through the PNAS open access option.

Data deposition: The sequence reported in this paper has been deposited in the GenBank database (accession no. GSE62611).

[1]X.D., T.L., and L.W. contributed equally to this work.

[2]To whom correspondence may be addressed. Email: cyliu@genetics.ac.cn or xfcao@genetics.ac.cn.

This article contains supporting information online at www.pnas.org/lookup/suppl/doi:10.1073/pnas.1522458113/-/DCSupplemental.

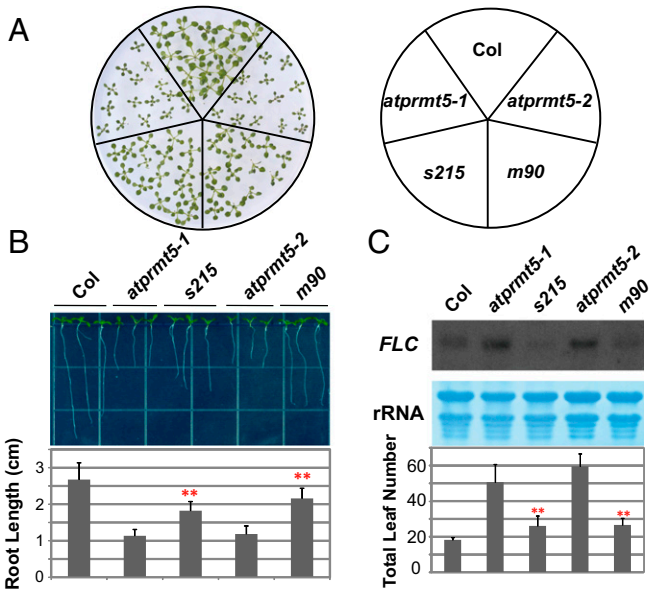

Fig. 1. *atprmt5* suppressors partially rescue the pleiotropic developmental defects of *atprmt5* mutants. (*A*) Rescued growth retardation of young seedling leaves at 12 d. (*B*) Rescued primary roots of *s215* and *m90* at 9 d. Data are shown as means ± SD ($n = 20$). Two-sided Student *t* test between *atprmt5* and the suppressors was performed (**$P < 0.01$). (*C*) Rescued *FLC* expression and flowering time of *s215* and *m90*. (*Upper*) The total RNAs from 12-d-old seedlings of Col, *atprmt5*, *s215*, and *m90* plants were probed by RNA blot with the full-length coding sequence of *FLC*. rRNAs were used as a loading control. (*Lower*) Flowering time was assessed by total leaf number after plants stopped producing new leaves when plants were grown at 23 °C under long day conditions. Data are shown as means ± SD ($n = 30$). Two-sided Student *t* test between *atprmt5* and the suppressors was performed (**$P < 0.01$).

developmental and splicing alterations of *atprmt5* mutants. Further study demonstrated that the Prp19C/NTC complex failed to be assembled into U5 snRNP to form activated spliceosome in *atprmt5* mutants, but was restored in the suppressor. We also showed that loss of symmetric arginine dimethylation on AtSm proteins in *atprmt5* failed to efficiently recruit Prp19C/NTC complex, which is essential for spliceosome activation. Our examination of the *atprmt5* phenotype and the interaction of *atprmt5* and *prp8* revealed an essential role for AtPRMT5 in spliceosome assembly and activation in pre-mRNA splicing.

Results

Two Suppressors Rescue the Pleiotropic Developmental Defects of *atprmt5* Mutants. Our previous study showed that *atprmt5* mutants exhibit pleiotropic phenotypes, such as dark green and curled leaves, growth retardation (9), and delayed flowering (9). To better understand the links connecting arginine methylation, post-transcriptional regulation, and plant development, and to identify the molecular mechanism by which AtPRMT5 functions in pre-mRNA splicing, we performed a genetic screen for suppressors of *atprmt5* mutants. *atprmt5-1* and *atprmt5-2* seeds were mutagenized with ethylmethane sulfonate (EMS), respectively, and individual M2 families were screened for mutations closed to the wild-type (WT) phenotypes. Among individual M2 families screened from *atprmt5* mutants, two allelic mutants, *s215* and *m90*, from *atprmt5-1* and *atprmt5-2*, respectively, partially rescued the pleiotropic phenotypes of *atprmt5* mutants. Compared with the *atprmt5* mutants, *s215* and *m90* plants showed less growth retardation, with larger cotyledons and longer primary roots than those of *atprmt5* mutants (Fig. 1 *A* and *B*). Intriguingly, compared with *atprmt5* mutants, the suppressors also showed partial suppression of the *atprmt5* delayed flowering phenotype, with decreased total leaf number (including rosette and cauline leaves) and *FLOWERING LOCUS C* (*FLC*) expression levels (Fig. 1*C*). In addition, the suppressors also showed less insensitivity to vernalization (Fig. S1*A*) and hypersensitivity to salt stress (Fig. S1*B*) compared with *atprmt5* mutants. Therefore, the two suppressors partially rescued the pleiotropic developmental defects of *atprmt5* mutants.

Point Mutations in Prp8 Are Responsible for Suppressors of *atprmt5* Mutants. Low-resolution mapping by bulked segregant analysis places *m90* and *s215* on the long arm of chromosome 1 between simple sequence length polymorphism (SSLP) markers 1-AC002986-9779 and 1-AC011713-9987 (2.5-cM), a region that covered 184 putative genes annotated in TAIR10 (Fig. S2*A*) (23). To identify the point mutations, we sequenced the genomic DNA of the F3 progeny of *m90* by Illumina Genome Analyzer *IIx*. Eleven homozygous SNPs were clustered in the region of chromosome 1 to where *m90* mapped (Table S1). A C3421T (nucleotide) transition mutation that is consistent with EMS mutagenesis was found, which changes a proline (P) to serine (S) at amino acid position 1,141 (P1141S) in the ORF of *At1g80070* (referred to from now as *prp8-8*; Fig. 2*A*), a locus involved in embryogenesis, as null mutants (*prp8-sus2* alleles) result in an abnormal suspensor development and embryonic lethality (24). Meanwhile, conventional DNA sequencing result showed that *s215*

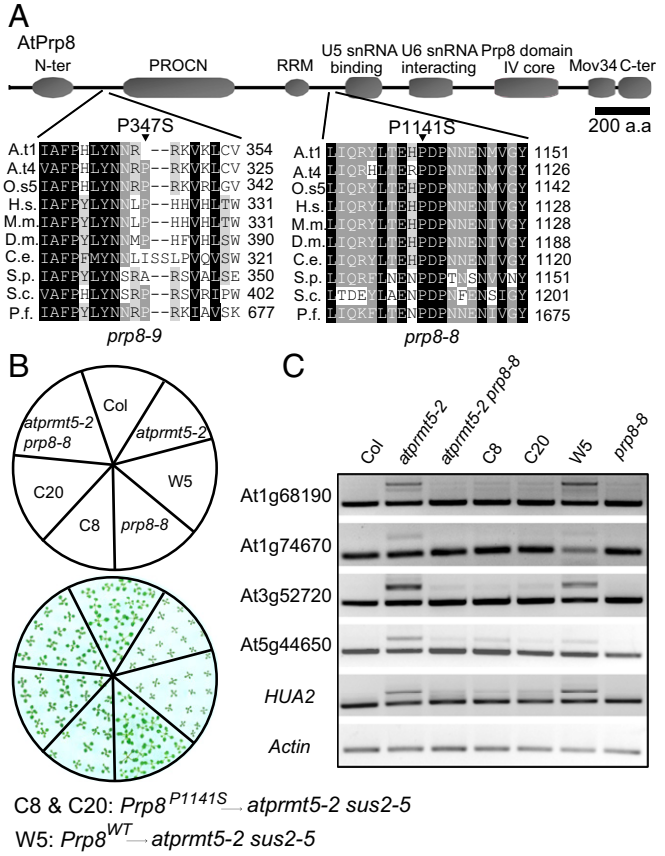

Fig. 2. Point mutations in Prp8 are responsible for suppressors of *atprmt5* mutants. (*A*) Sequence alignment of the conserved Prp8 containing the P347S and P1141S mutations in *prp8-9* and *prp8-8*, respectively. Abbreviations for species are as follows: *Arabidopsis thaliana* (At), *Oryza sativa* (Os), *Homo sapiens* (Hs), *Mus musculus* (Mm), *Drosophila melanogaster* (Dm), *Caenorhabditis elegans* (Ce), *Schizosaccharomyces pombe* (Sp), *Saccharomyces cerevisiae* (Sc), and *Plasmodium falciparum* (Pf). The point mutation sites are labeled by black triangles. (*B* and *C*) Rescued growth retardation of young seedling leaves at 12 d (*B*) and intron retention events (*C*) by a transformation of CDS *Prp8* clone with P1141S mutation in *atprmt5-2 sus2-5* double mutants background. C8 and C20 are two individual transgenic lines containing P1141S construct of Prp8. W5 is the control transgenic line containing WT Prp8 construct.

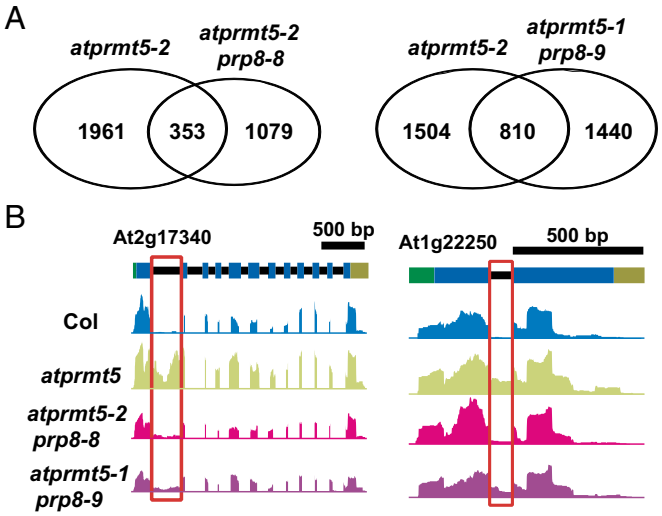

Fig. 3. *atprmt5* suppressors partially rescue the splicing alterations of *atprmt5* mutants. (*A*) Overlapping analysis of significantly altered constitutive splicing events between *atprmt5-2* and the suppressors. (*B*) Two examples of intron retention events rescued in *atprmt5-1 prp8-9* and *atprmt5-2 prp8-8*. Annotated gene structures are shown (*Upper*), with thick lines representing exons and thin lines representing introns. Wiggle plots representing the normalized reads coverage in a logarithmic scale (log_2) are shown in blue for Col, in green for *atprmt5* mutants, in pink for *atprmt5-2 prp8-8*, and in purple for *atprmt5-1 prp8-9*. The red frames indicate the retained introns rescued in *atprmt5-1 prp8-9* and *atprmt5-2 prp8-8*.

carried P347S substitution in *At1g80070* as well (referred to from now as *prp8-9*) (Fig. 2*A*). *prp8-8* and *prp8-9* are neomorphic alleles of *Prp8*, because neither *prp8-6* (also named *sof81, a* hypomorphic mutant allele of *Prp8*) (25) nor *Prp8* RNAi lines rescue the splicing alterations of *atprmt5* mutants (Fig. S1*C*). In addition, the rescued phenotypes and splicing alterations in *atprmt5 prp8* plants were mimicked by a coding sequence (CDS) of *Prp8* clone with P1141S mutation, but not without mutation, in *atprmt5-2 sus2-5* double mutants (Fig. 2 *B* and *C* and Fig. S1*D*), indicating that the neomorphic mutation of *Prp8* can rescue the pleiotropic phenotypes of *atprmt5* mutants. However, there is no obvious physiological and molecular effect in *prp8-8* and *prp8-9* single mutants compared with wild-type Col (Fig. 2 *B* and *C* and Fig. S1 *E*–*G*).

At1g80070 encodes the *Arabidopsis* homolog of the highly conserved U5 snRNP component (26), Prp8, which plays a central role in the catalytic core of the spliceosome and is highly conserved from yeast to plants and humans (27) (Fig. S2*B*). A recent study showed that *Arabidopsis* Prp8 is involved in modulating the splicing of the GFP reporter gene in a genetic screen (28) and long noncoding transcript *COOLAIR* to regulate *FLC* transcription (25). Protein sequence alignment of Prp8 homologs showed that P1141 of Prp8 is in the linker region between the RNA recognition motif (RRM) and the U5-snRNA binding domain and is highly conserved from yeast to humans, and P347 is in the linker region between the N-terminal domain and the PROCN domain and is moderately conserved (Fig. 2*A*). These mutations neither cause a change in Prp8 protein levels nor affect the subcellular localization of Prp8 in *Arabidopsis* (Fig. S3*A*). AtPRMT5 could neither methylate nor interact with Prp8 (Fig. S3 *B* and *C*).

The Suppressors Partially Rescue the Splicing Alterations of *atprmt5* Mutants. To test whether *atprmt5-1 prp8-9* and *atprmt5-2 prp8-8* restore the splicing alterations genome-wide, we performed ultrahigh-throughput RNA sequencing (RNA-seq) to examine the global pre-mRNA splicing (Table S2). Compared with Col, we identified 2,314 intron retention events in *atprmt5* mutants. By contrast, we found that 84.7% (1,961 of 2,314) intron retention events in *atprmt5-2 prp8-8* and 65.0% (1,504 of 2,314) in *atprmt5-1 prp8-9* ($P < 0.01$) were rescued, respectively (Fig. 3*A* and Fig. S4*A*). Fig. 3*B* shows two examples of mRNAs with rescued intron retention events detected by RNA-seq. In addition, we analyzed alternative splicing (AS) events and identified 348 decreased and 416 increased AS events in *atprmt5* mutants, among which 62% (216 of 348) and 55% (193 of 348) of decreased AS events, and 76% (316 of 416) and 62% (257 of 416) of increased AS events were rescued in *atprmt5-2 prp8-8* and *atprmt5-1 prp8-9*, respectively (Fig. S4*B*).

Moreover, we also compared the 5′ splice-site sequence in *atprmt5* and *atprmt5-2 prp8-8* (including rescued events and nonrescued events) compared with the 5′ splice-site consensus sequence of all introns present in the *Arabidopsis* genome. Compared with the *Arabidopsis* 5′ splice-site consensus sequence (Fig. S4*C*, first panel), *atprmt5* displayed a significant decrease in the frequency of the dominant consensus G and A at the −1 and −2 positions, respectively, and a tendency toward randomization of the nucleotides at the +5 positions (Fig. S4*C*, second panel), consistent with the previous results from Yanovsky's laboratory (10, 12). Then we compared the 5′ splice-site sequence in the rescued and nonrescued splicing events in *atprmt5-2 prp8-8* and found that the nonrescued splicing events in *atprmt5-2 prp8-8* showed a more tendency toward randomization of the nucleotides at the −3, −2, and −1 positions (Fig. S4*C*, third and fourth panels), suggesting that the P1141S point mutation is more inclined to rescue the intron retention events with less random 5′ splice-site in *atprmt5*. These results showed that the suppressors partially rescued the constitutive and alternative splicing alterations of *atprmt5* mutants, consistent with their recovered developmental phenotypes. Because of the higher conservation of the affected amino acid, and the higher rescued splicing alterations efficiency in the mutant plants, we used *atprmt5-2 prp8-8* (*m90*) for the following studies.

Prp19C/NTC and Step-Specific Splicing Factors Fail to Incorporate into the Spliceosomal Core in *atprmt5* Mutants. The highly dynamic spliceosome changes in composition and conformation during complex assembly, catalytic activation, active site remodeling, and complex disassembly, providing accuracy and flexibility in pre-mRNA splicing (15, 29). Prp8, a highly conserved and essential component of the U5 snRNP, occupies a central position in the catalytic core of the spliceosome, interacts with the pre-mRNA, U snRNA, and numerous protein factors, and has been implicated in several structural and compositional rearrangements during splicing (27). The recently reported crystal structure of yeast Prp8 reveals that the mutated amino acid in *prp8-8* occurs on the outer surface of Prp8, which may affect interactions with surrounding components within the spliceosome (30). Therefore, we hypothesized that AtPRMT5 may be required for proper complex composition during spliceosome formation and activation, and the neomorphic mutation of *atprmt5-2 prp8-8* might overcome the requirement for AtPRMT5.

To explore the alterations of spliceosome composition in *atprmt5* mutants, we characterized Prp8-associated proteins by MS. We extracted nuclear proteins from Col, *atprmt5-2*, *atprmt5-2 prp8-8*, and *prp8-8* plants and immunoprecipitated with anti-Prp8 antibodies, and then used MS to identify the components that interact with Prp8. We used spectral counts to quantify protein abundance in various spliceosomal complexes and normalized the counts for each protein to the spectral counts for Prp8 to estimate the relative abundance of proteins associating with Prp8. We identified 477 proteins that each had more than five spectral counts. Gene Ontology (GO) analysis revealed that these interacting proteins function in multiple biological processes (Fig. S5*A*).

Intriguingly, among the proteins that interact with Prp8, our MS results identified a set of splicing factors, which form the Prp19 complex (Prp19C), also known as NTC (21, 31, 32). Compared with Col, the *atprmt5* mutants showed significantly reduced normalized spectral counts from the Prp19C/NTC core proteins, including MAC3A and MAC3B (human Prp19 homolog in *Arabidopsis*), MOS4 (human SPF27 homolog in *Arabidopsis*), CDC5, and PRL1, and the Prp19C/NTC-associated proteins (SYF1, AQR, CRN1c, SKIP, ECM2, ISY1, and PPI) (Fig. 4*A*, *Upper*, and Table S3), suggesting that Prp19C/NTC cannot efficiently interact with Prp8 in

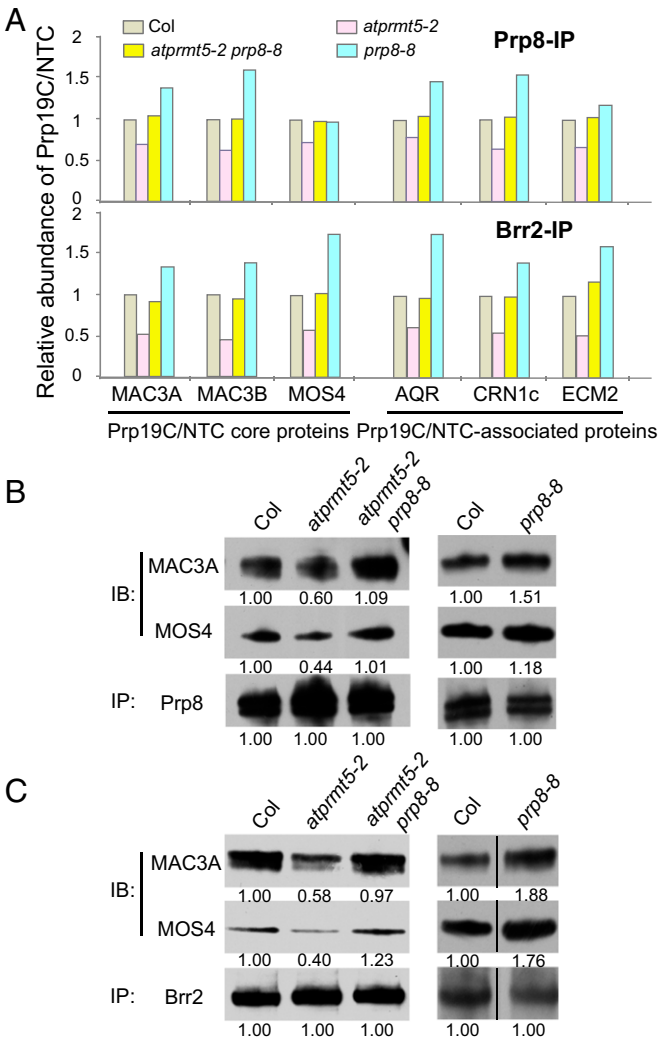

Fig. 4. The recruitment of Prp19C/NTC to the spliceosome is impaired in *atprmt5* mutants and restored in *atprmt5-2 prp8-8*. (*A*) The association of Prp19C/NTC and Prp8 (and Brr2) decreased in *atprmt5* mutants and was rescued in *atprmt5-2 prp8-8* mutants. Nuclear extracts from Col, *atprmt5-2*, *atprmt5-2 prp8-8*, and *prp8-8* were immunoprecipitated by anti-Prp8 (*Upper*) and anti-Brr2 (*Lower*) polyclonal antibodies, and the interacting proteins were identified by MS. The spectral counts of Prp19C/NTC from *atprmt5-2*, *atprmt5-2 prp8-8*, and *prp8-8* were divided by that from Col, and the ratios are shown in the histogram. (*B* and *C*) Prp8- or Brr2-associated proteins were identified in Col, *atprmt5*, *atprmt5-2 prp8-8*, and *prp8-8* by MS. Prp8 (*B*) and Brr2 (*C*) were immunoprecipitated by anti-Prp8 and anti-Brr2 antibodies, respectively, and immunoblotting was performed with anti-MAC3A and anti-MOS4 antibodies for Prp19C/NTC. The dividing lines in *C*, *Right* indicate noncontiguous images between Col and *prp8-8*.

atprmt5 mutants. *atprmt5-2 prp8-8* showed restored counts for these Prp19C/NTC core proteins, whereas *prp8-8* displayed a slightly increased interaction with Prp19C/NTC (Fig. 4*A*, *Upper*, and Table S3), indicating that the Prp8^{P1141S} version can restore the pre-mRNA splicing defects of *atprmt5* mutants by increased recruiting Prp19C/NTC to the spliceosome core. To further substantiate the MS results, immunoprecipitation of nuclear extracts with anti-Prp8 antibodies in Col, *atprmt5-2*, *atprmt5-2 prp8-8*, and *prp8-8*, followed by immunoblotting with anti-MAC3A and anti-MOS4 antibodies revealed the decreased interaction of Prp8 with Prp19C/NTC in *atprmt5-2* mutants, and the restored interaction in *atprmt5-2 prp8-8* mutants, which are independent of RNA (Fig. S5*B*) and consistent with the MS results (Fig. 4*B*).

As an integral component of active spliceosome, Prp19C/NTC associates with the spliceosome during pre-mRNA splicing and participates in modulating spliceosome composition and conformation (22). In addition to the Prp19C/NTC components, we also found that *atprmt5-2* mutants showed decreased association between Prp8 and the specific splicing factors in the first (Prp2, Cwf21, and CWC22) and the second (Prp17 and Prp22) catalytic steps; these associations were recovered in *atprmt5-2 prp8-8* mutants (Table S3). These results suggest that AtPRMT5 is required for the recruitment of Prp19C/NTC and specific splicing factors to the catalytic core of the spliceosome, which is essential for spliceosome activation.

To verify that Prp19C/NTC cannot be efficiently recruited to the spliceosome core in *atprmt5* mutants, we immunoprecipitated Brr2, a DEAH-box ATPase that interacts with Prp8 (Fig. S5*C*), and used MS to identify the components that interacted with Brr2. We identified 336 proteins, 277 of which overlapped with Prp8-associated components ($P = 2.36 \times 10^{-13}$; Fig. S5*D*). Consistent with our Prp8 results, the interactions between Brr2 and Prp19C/NTC, the specific splicing factors in the first and second catalytic steps, decreased in *atprmt5* mutants, but were restored in *atprmt5-2 prp8-8* (Fig. 4 *A*, *Lower*, and *C* and Table S3), supporting the idea that AtPRMT5 deficiency impairs the interaction between Prp19C/NTC and the spliceosome core and suggesting the essential role for AtPRMT5 in activating the spliceosome.

Prp19C/NTC Recruitment to the Spliceosome Requires Symmetric Dimethylation of AtSm Proteins. Our previous study showed that AtPRMT5 symmetrically di-methylates AtSmD1, D3, and AtLSm4 proteins, which form the basic core components of U snRNP and have essential functions in splicing (11). To distinguish the methylation status of these AtSm proteins, we used low complex GAR motifs harboring SDMA as the antigen to generate antibodies that specifically detect these methylation marks (Fig. S6*A*). To characterize the antibody, we tested it on total proteins from Col and *atprmt5* mutants. We observed that the signal recognized by the SDMA-specific antibody (mainly AtSmD1 and AtSmD3) dramatically decreased in *atprmt5* mutants (Fig. S6*B*), suggesting that AtPRMT5 is responsible for symmetric dimethylation of arginine residues of AtSm proteins in vivo.

To better understand the role of these symmetrically dimethylated AtSm proteins in spliceosome assembly, we first used size exclusion chromatography to analyze their elution profiles in extracts from Col. We observed that the symmetrically dimethylated AtSm proteins (mainly AtSmD1 and AtSmD3) roughly distributed into two peaks, which we termed complex I (larger than 669 kDa, fractions 2–8) and complex II (around 669 kDa, fractions 11–16), supported by U snRNA profiles (Fig. 5*A*). To examine the protein composition of complex I and complex II, we combined the corresponding eluted fractions, immunoprecipitated with SDMA antibody, and used MS to identify the protein components. Among the protein components identified, complex I contained U2, U5, and U6 snRNPs, and Prp19C/NTC; complex II contained U1 and U2 snRNPs (Fig. 5*B*). The partial composition analysis suggests that complex I and complex II are more consistent with activated and preactivated forms of the spliceosome, respectively.

AtSmD3 stably exists in U1, U2, U4, and U5 snRNPs, and is involved in almost every state of the spliceosome during pre-mRNA splicing. To explore whether the symmetrical di-methylation of Sm core proteins affects spliceosome assembly and activation, we collected complex I fractions from Col, *atprmt5-2*, *atprmt5-2 prp8-8*, and *prp8-8*, and then performed immunoprecipitation with anti-AtSmD3b antibodies, followed by immunoblotting with anti-MAC3A and anti-MOS4 antibodies. The results further confirmed the decreased interaction between AtSmD3b and Prp19C/NTC in *atprmt5-2* mutants, which was restored in *atprmt5-2 prp8-8* (Fig. 5*C*), consistent with the Prp8 IP-MS results, again verifying that Prp19C/NTC cannot be efficiently recruited to the activated spliceosome, which leads to the constitutive and alternative splicing alterations in *atprmt5* mutants.

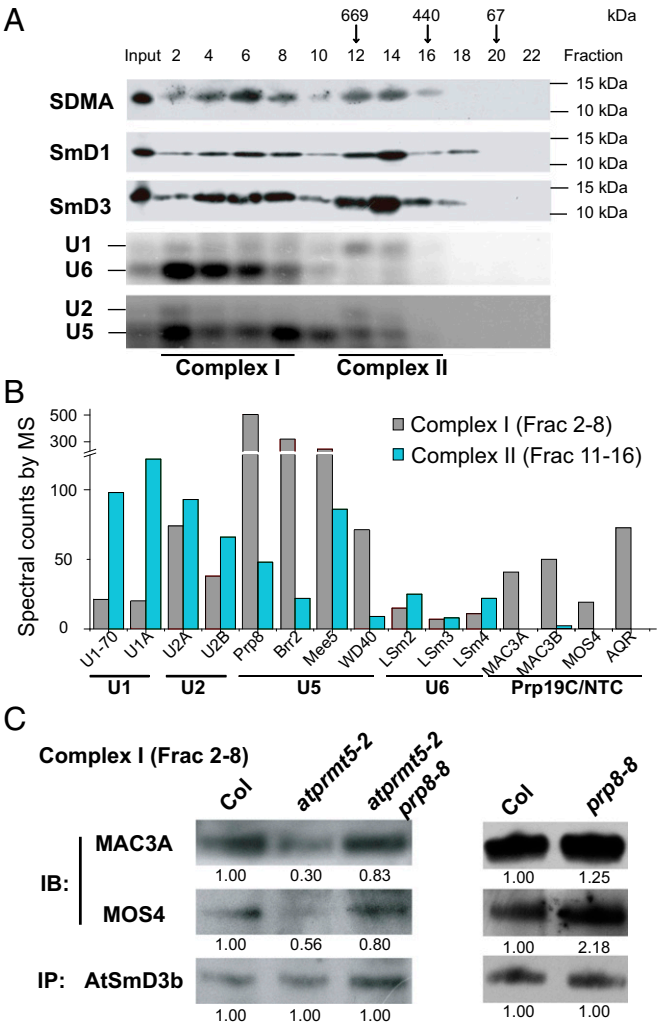

Fig. 5. Decreased recruitment of Prp19C/NTC to the spliceosome in *atprmt5* mutants. (*A*) The elution profiles of symmetric dimethylated AtSmD1 and AtSmD3 proteins. Cell lysates from Col were fractionated by gel filtration chromatography as described in *Materials and Methods* and were immunoblotted to visualize symmetric dimethylated AtSmD1 and AtSmD3. The molecular weights of the calibration standards and their elution positions are indicated. (*B*) The distribution of the spliceosomal proteins in gel filtration chromatography. Fractions 2–8 and 11–16 were collected and immunoprecipitated with SDMA antibody, and then the associated proteins were identified by MS. The spectral counts of U snRNPs and Prp19C/NTC are shown in the histogram. (*C*) The interaction status between AtSmD3b and Prp19C/NTC in complex I. Fractions 2–8 were collected from Col, *atprmt5-2*, *atprmt5-2 prp8-8*, and *prp8-8*, and AtSmD3b was immunoprecipitated by anti-AtSmD3b polyclonal antibody, and then immunoblotting was performed with anti-MAC3A and anti-MOS4 polyclonal antibodies for Prp19C/NTC and anti-AtSmD3b antibody for loading controls.

Discussion

Extensive studies have shown that PRMT5 deficiency produces diverse phenotypes in different organisms. We and others have demonstrated that AtPRMT5 is essential for constitutive and alternative pre-mRNA splicing of diverse genes, but how AtPRMT5 functions in pre-mRNA splicing has remained unclear (10–12, 33). Here we showed that AtPRMT5 promotes the recruitment of Prp19C/NTC and key first step and second step splicing factors to the spliceosome, thus enabling global pre-mRNA splicing under normal growth conditions (Fig. S6*D*).

PRMT5 can symmetrically dimethylate the C-terminal tails of the U snRNP Sm proteins B/B′, D1, D3, and LSm4 in multiple organisms, which may facilitate the recognition of a subset of 5′ splice sites (10, 11, 33–36). Here *atprmt5* mutants show a dramatic impairment of the interaction between Prp19C/NTC and AtSmD3b, revealing a previously unidentified function of symmetric arginine dimethylation in the recruitment of Prp19C/NTC to the spliceosome. In the Prp8 and Brr2 IP-MS data, it is interesting to find that the interactions between Prp8/Brr2 and the components in U2 and U6 snRNP, but not in U5 snRNP (Fig. S5 *E* and *F*), decreased in *atprmt5* mutants, and were partially restored in *atprmt5-2 prp8-8*, suggesting the defects of spliceosome assembly to the introns in *atprmt5* mutants. Although the U snRNAs (including U1, U2, U4, U5, and U6 snRNAs) levels were significantly increased in *atprmt5* mutants (Fig. S6*C*), it cannot rescue the splicing alterations, reflecting a feedback of impaired spliceosome assembly in some of introns in *atprmt5*. The crystal structure of yeast Prp8 shows that the conserved proline mutated in *prp8-8* is located on the outer surface of the RT/En domain, a crucial protein-binding surface, which may affect interactions with surrounding components within the spliceosome (30), and the increased interaction between U5 snRNP with $Prp8^{P1141S}$ and Prp19C/NTC in *prp8-8* mutants proved this structural hypothesis. Because AtPRMT5 deficiency results in inefficient recruitment of Prp19C/NTC to the spliceosome, it makes sense that the $Prp8^{P1141S}$ version can restore the pre-mRNA splicing defects in *atprmt5* mutants by increased recruiting Prp19C/NTC to the spliceosome core. We therefore hypothesized that, in *atprmt5* mutants, the loss of symmetric arginine dimethylation of Sm core proteins alters their binding interactions with other spliceosomal components by changing protein surface structure and hydrophobicity. Mutations in Prp8 may slightly reposition its interacting proteins within the spliceosome to facilitate the optimization of conformation, thereby reversing the splicing alterations in *atprmt5* (Fig. S6*D*).

RNA splicing is a critical posttranscriptional regulatory mechanism, and ∼60% of noninfectious human diseases arise from splicing disorders; thus, the study of pre-mRNA splicing mechanisms has a high priority for human health (37). Splicing involves highly dynamic, organized, and exceptional compositional and structural rearrangements within the spliceosome during complex assembly, catalytic activation, and disassembly (38). Therefore, any mutations in the genes involved in RNA splicing machinery may give rise to serious diseases (37). For example, perturbation of the *SMN* gene results in widespread splicing defects and thus causes spinal muscular atrophy, a motor neuron disease (39). Despite increasing evidence showing that PRMT5 deficiency leads to genome-wide splicing alterations in different species, our study is the first attempt, to our knowledge, to dissect the underlying mechanism, showing that AtPRMT5 is indispensable for the recruitment of Prp19C/NTC and splicing factors in the catalytic reactions to the spliceosome and a potential conserved mechanism for PRMT5 in pre-mRNA splicing. Additionally, PRMT5 deficiency is (at least in part) involved in Huntington's disease pathogenesis (40), whereas PRMT5 overexpression occurs in a large number of cancers (41). Thus, PRMT5 plays multifarious roles in human diseases. Due to the evolutionary conservation of PRMT5 in different species, our findings provide a fundamental molecular mechanism applicable to all eukaryotes, thereby shedding light on PRMT5 functions and spliceosome activation in animals.

Materials and Methods

Plant Materials. The *atprmt5-1* and *atprmt5-2* mutants were characterized previously (9), and *atprmt5-2 prp8-8* and *atprmt5-1 prp8-9* were isolated in this study. Further details can be found in *SI Materials and Methods*.

RNA Sequencing and Data Analysis. Total RNA was subjected to polyA selection (Invitrogen), and strand-specific RNA-seq libraries were constructed using SMART method (42). The data analysis method was according to the previously reported method (11, 12). RT-PCR is performed using intron-flanking primers (Table S4) for validation. Further details can be found in *SI Materials and Methods*.

Proteomic Analysis. Affinity purified protein complexes were separated on a 4–12% Bis-Tris gel (Life Technologies), and the proteins bands were subjected

to in-gel digestion as described previously (43). Further details can be found in *SI Materials and Methods*.

Additional methods are available in *SI Materials and Methods*.

ACKNOWLEDGMENTS. We thank Dr. Haiyan Zheng (Rutgers University) for conducting the MS analysis, Dr. Caroline Dean for providing *prp8-6* seeds, Dr. Marcelo J. Yanovsky for sharing the data analysis pipelines, and the *Arabidopsis* Biological Resource Center for providing SALK T-DNA insertion lines. This work was supported by National Natural Science Foundation of China Grants 31330020 and 31210103901 (to X.C.), 31200900 (to X.D.), and 31370770 (to C.L.), National Basic Research Program of China Grant 2011CB915401 (to X.C.), and the State Key Laboratory of Plant Genomics.

1. Sun L, et al. (2011) Structural insights into protein arginine symmetric dimethylation by PRMT5. *Proc Natl Acad Sci USA* 108(51):20538–20543.
2. Ahmad A, Cao X (2012) Plant PRMTs broaden the scope of arginine methylation. *J Genet Genomics* 39(5):195–208.
3. Liu C, Lu F, Cui X, Cao X (2010) Histone methylation in higher plants. *Annu Rev Plant Biol* 61:395–420.
4. Bedford MT, Clarke SG (2009) Protein arginine methylation in mammals: Who, what, and why. *Mol Cell* 33(1):1–13.
5. Yang M, et al. (2009) Caenorhabditis elegans protein arginine methyltransferase PRMT-5 negatively regulates DNA damage-induced apoptosis. *PLoS Genet* 5(6):e1000514.
6. Wrighton KH (2011) Cell signalling: PRMT5 restricts ERK activity. *Nat Rev Mol Cell Biol* 12(11):689.
7. Ancelin K, et al. (2006) Blimp1 associates with Prmt5 and directs histone arginine methylation in mouse germ cells. *Nat Cell Biol* 8(6):623–630.
8. Tee WW, et al. (2010) Prmt5 is essential for early mouse development and acts in the cytoplasm to maintain ES cell pluripotency. *Genes Dev* 24(24):2772–2777.
9. Pei Y, et al. (2007) Mutations in the Type II protein arginine methyltransferase AtPRMT5 result in pleiotropic developmental defects in Arabidopsis. *Plant Physiol* 144(4):1913–1923.
10. Sanchez SE, et al. (2010) A methyl transferase links the circadian clock to the regulation of alternative splicing. *Nature* 468(7320):112–116.
11. Deng X, et al. (2010) Arginine methylation mediated by the Arabidopsis homolog of PRMT5 is essential for proper pre-mRNA splicing. *Proc Natl Acad Sci USA* 107(44):19114–19119.
12. Hernando CE, Sanchez SE, Mancini E, Yanovsky MJ (2015) Genome wide comparative analysis of the effects of PRMT5 and PRMT4/CARM1 arginine methyltransferases on the Arabidopsis thaliana transcriptome. *BMC Genomics* 16:192.
13. Zhang Z, et al. (2011) Arabidopsis floral initiator SKB1 confers high salt tolerance by regulating transcription and pre-mRNA splicing through altering histone H4R3 and small nuclear ribonucleoprotein LSM4 methylation. *Plant Cell* 23(1):396–411.
14. Green MR (1986) Pre-mRNA splicing. *Annu Rev Genet* 20:671–708.
15. Wahl MC, Will CL, Lührmann R (2009) The spliceosome: Design principles of a dynamic RNP machine. *Cell* 136(4):701–718.
16. Brahms H, Meheus L, de Brabandere V, Fischer U, Lührmann R (2001) Symmetrical dimethylation of arginine residues in spliceosomal Sm protein B/B′ and the Sm-like protein LSm4, and their interaction with the SMN protein. *RNA* 7(11):1531–1542.
17. Friesen WJ, et al. (2001) The methylosome, a 20S complex containing JBP1 and pICln, produces dimethylarginine-modified Sm proteins. *Mol Cell Biol* 21(24):8289–8300.
18. Meister G, Fischer U (2002) Assisted RNP assembly: SMN and PRMT5 complexes cooperate in the formation of spliceosomal UsnRNPs. *EMBO J* 21(21):5853–5863.
19. Neuenkirchen N, Chari A, Fischer U (2008) Deciphering the assembly pathway of Sm-class U snRNPs. *FEBS Lett* 582(14):1997–2003.
20. Gao X, et al. (2012) Tudor staphylococcal nuclease (Tudor-SN) participates in small ribonucleoprotein (snRNP) assembly via interacting with symmetrically dimethylated Sm proteins. *J Biol Chem* 287(22):18130–18141.
21. Chanarat S, Sträßer K (2013) Splicing and beyond: The many faces of the Prp19 complex. *Biochim Biophys Acta* 1833(10):2126–2134.
22. Matera AG, Wang Z (2014) A day in the life of the spliceosome. *Nat Rev Mol Cell Biol* 15(2):108–121.
23. Hou X, et al. (2010) A platform of high-density INDEL/CAPS markers for map-based cloning in Arabidopsis. *Plant J* 63(5):880–888.
24. Schwartz BW, Yeung EC, Meinke DW (1994) Disruption of morphogenesis and transformation of the suspensor in abnormal suspensor mutants of Arabidopsis. *Development* 120(11):3235–3245.
25. Marquardt S, et al. (2014) Functional consequences of splicing of the antisense transcript COOLAIR on FLC transcription. *Mol Cell* 54(1):156–165.
26. Lossky M, Anderson GJ, Jackson SP, Beggs J (1987) Identification of a yeast snRNP protein and detection of snRNP-snRNP interactions. *Cell* 51(6):1019–1026.
27. Grainger RJ, Beggs JD (2005) Prp8 protein: At the heart of the spliceosome. *RNA* 11(5):533–557.
28. Sasaki T, et al. (2015) An Rtf2 domain-containing protein influences pre-mRNA splicing and is essential for embryonic development in Arabidopsis thaliana. *Genetics* 200(2):523–535.
29. Yan C, et al. (2015) Structure of a yeast spliceosome at 3.6-angstrom resolution. *Science* 349(6253):1182–1191.
30. Galej WP, Oubridge C, Newman AJ, Nagai K (2013) Crystal structure of Prp8 reveals active site cavity of the spliceosome. *Nature* 493(7434):638–643.
31. Koncz C, Dejong F, Villacorta N, Szakonyi D, Koncz Z (2012) The spliceosome-activating complex: Molecular mechanisms underlying the function of a pleiotropic regulator. *Front Plant Sci* 3:9.
32. Wang BB, Brendel V (2004) The ASRG database: Identification and survey of Arabidopsis thaliana genes involved in pre-mRNA splicing. *Genome Biol* 5(12):R102.
33. Bezzi M, et al. (2013) Regulation of constitutive and alternative splicing by PRMT5 reveals a role for Mdm4 pre-mRNA in sensing defects in the spliceosomal machinery. *Genes Dev* 27(17):1903–1916.
34. Chari A, et al. (2008) An assembly chaperone collaborates with the SMN complex to generate spliceosomal SnRNPs. *Cell* 135(3):497–509.
35. Zhang D, Abovich N, Rosbash M (2001) A biochemical function for the Sm complex. *Mol Cell* 7(2):319–329.
36. Weber G, Trowitzsch S, Kastner B, Lührmann R, Wahl MC (2010) Functional organization of the Sm core in the crystal structure of human U1 snRNP. *EMBO J* 29(24):4172–4184.
37. Wang J, Zhang J, Li K, Zhao W, Cui Q (2012) SpliceDisease database: Linking RNA splicing and disease. *Nucleic Acids Res* 40(Database issue):D1055–D1059.
38. Valadkhan S (2011) A snRNP's ordered path to maturity. *Genes Dev* 25(15):1563–1567.
39. Zhang Z, et al. (2008) SMN deficiency causes tissue-specific perturbations in the repertoire of snRNAs and widespread defects in splicing. *Cell* 133(4):585–600.
40. Ratovitski T, Arbez N, Stewart JC, Chighladze E, Ross CA (2015) PRMT5- mediated symmetric arginine dimethylation is attenuated by mutant huntingtin and is impaired in Huntington's disease (HD). *Cell Cycle* 14(11):1716–1729.
41. Stopa N, Krebs JE, Shechter D (2015) The PRMT5 arginine methyltransferase: Many roles in development, cancer and beyond. *Cell Mol Life Sci* 72(11):2041–2059.
42. Levin JZ, et al. (2010) Comprehensive comparative analysis of strand-specific RNA sequencing methods. *Nat Methods* 7(9):709–715.
43. Rappsilber J, Mann M (2007) Analysis of the topology of protein complexes using cross-linking and mass spectrometry. *CSH Protoc* 2007(2):4594.
44. Trapnell C, Pachter L, Salzberg SL (2009) TopHat: Discovering splice junctions with RNA-Seq. *Bioinformatics* 25(9):1105–1111.
45. Langmead B, Trapnell C, Pop M, Salzberg SL (2009) Ultrafast and memory-efficient alignment of short DNA sequences to the human genome. *Genome Biol* 10(3):R25.